STM of Insulators with the Probe in Contact with an Aqueous Layer

Nikin Patel,* Martyn C. Davies, Martin Lomas, Clive J. Roberts, Saul J. B. Tendler, and Philip M. Williams

Laboratory of Biophysics and Surface Analysis, Department of Pharmaceutical Sciences, The University of Nottingham, Nottingham NG7 2RD, U.K.

Received: November 13, 1996; In Final Form: April 14, 1997[⊗]

The advent of scanning tunneling microscopy of electrical insulators and biological specimens has raised significant questions as to the mechanisms involved in image formation. We show that for successful high-resolution imaging of hydrated films of two different proteins, a water bridge can exist between the tunneling microscope probe and the sample surface. Current−probe/sample separation plots on hydrated and dehydrated protein confirm the formation of a water bridge. The practical realization of these results are discussed.

Introduction

A robust understanding of the mechanism of image contrast formation is critical to the utilization of the scanning tunneling microscope (STM) in the study of biomolecular structure and function. A number of groups, including ourselves, have shown that the hydration state of insulating samples such as biomolecules has a direct effect on STM image contrast.[1−6] Nevertheless, controversy remains over the mechanism of image contrast formation, in particular, whether the STM tip penetrates the adsorbed surface water present on hydrated samples. Yuan *et al.*[7] first proposed that when samples are covered with a thin film of water, the measured current is carried by ions rather than tunneling electrons. Fan and Bard[1] recently proposed STM imaging on wet insulators as utilizing an electrochemical mechanism of conduction with the apex of the STM tip being maintained in contact with an ultrathin water layer. In contrast, Guckenberger and co-workers propose a direct electronic tunneling mechanism without the STM tip touching the adsorbed surface water.[2,8] We further this debate by showing that, under the imaging conditions employed here, the STM tip directly contacts the surface water of a hydrated sample. This is clearly demonstrated by the repeated imaging of two different protein monolayers under hydrated, dehydrated, and rehydrated conditions.

Experimental Section

The protein immobilization strategy we have employed has been described previously.[3] Briefly, a coupling reagent, *N*-succinimidyl-3-(2-pyridyldithio)propionate (SPDP) (Pierce, Luton, U.K.) was dissolved in anhydrous 2,2,2-trifluoroethanol (TFE) (99%+, Aldrich, Gillingham, Dorset, U.K.) to a concentration of 12 mM. Epitaxially grown gold films on mica were then immersed in the SPDP solution for a period of 5 h to create a functionalized self-assembled monolayer.[3,9] The samples were then transferred to a solution containing either approximately 0.4 μM catalase (Sigma, Poole, Dorset, U.K.) or 7 μM fibrinogen (Sigma, U.K.) in TFE. The same volume of *N*,*N*-diisopropylethylamine (DIPEA, 99.5%, Aldrich, Dorset, U.K.) was then added. The gold was incubated in these solutions for 21 h and washed exhaustively in flowing deionized water in order to remove any noncovalently bound protein. The samples were then imaged in a variable humidity chamber with platinum−iridium tips using a VG STM 2000 system (VG Microtech, Uckfield, U.K.). Typical experimental conditions comprised a current of 40 pA and a tip bias voltage range of −1.13 to +1.13 V. The relative humidity (R.H.) of each sample atmosphere was controlled using saturated sodium chloride solutions for hydrating the sample and a mixture of freshly generated 3 Å molecular sieves and silica gel for dehydration. The humidity of the chamber was routinely checked using a humidity meter (Vaisala HMI 31, R.S. Components, Corby, Northhants, U.K.) housed inside the chamber.

Results and Discussion

Figure 1A displays an image of a monolayer of catalase recorded in a high-humidity environment (76% R.H.). Individual molecules are clearly resolved with an observed diameter of approximately 10 nm and a height of 6 nm, which corresponds with dimensions obtained from X-ray crystallography (10.5 nm × 10.5 nm × 6 nm),[10] although depending on the orientation of the catalase molecules on the surface, the height could in theory be 6−10.5 nm. STM height measurements of hydrated biomolecules can be variable and are strongly dependent on a given tip, humidity, tunneling current, and voltage.[6] Here, we demonstrate that the dehydration of the environment produces no change in image contrast (Figure 1B) when the tip remains in contact with the surface with maintenance of the imaging current. However, if the tip is then retracted by approximately 500 nm and immediately lowered (Figure 1C), image contrast is significantly reduced with individual molecules barely discernible. On rehydration, there is only a modest improvement in image contrast when the tip remains in place (Figure 1D). Significant improvement of the image quality to original levels only occurs after the tip is again withdrawn and lowered (Figure 1E).

These changes in image contrast which result after tip retraction and lowering clearly indicate an interaction between the STM tip and adsorbed surface water (see Figure 1F−J). We propose that, in a hydrated environment, the tip penetrates a water film adsorbed to the protein monolayer (Figure 1F). On dehydration of the environment, a water bridge remains due to capillary forces, between the tip and the surface (Figure 1G), and is able to remain stable despite lowering of the relative humidity.[11] Tip retraction results in the breakage of this bridge which fails to reform on lowering (Figure 1H). Due to the reduction in conductivity of the sample, the tip−sample separation may decrease with the tip contacting the catalase monolayer. This may account for the appearance of Figure 1C; however,

* Corresponding author. E-mail address: paxnp@unix.ccc.nottingham.ac.uk. Telephone: +44 (0) 115 9515063. Fax: +44 (0) 115 9515110.

[⊗] Abstract published in *Advance ACS Abstracts,* June 1, 1997.

S1089-5647(96)03787-X CCC: $14.00

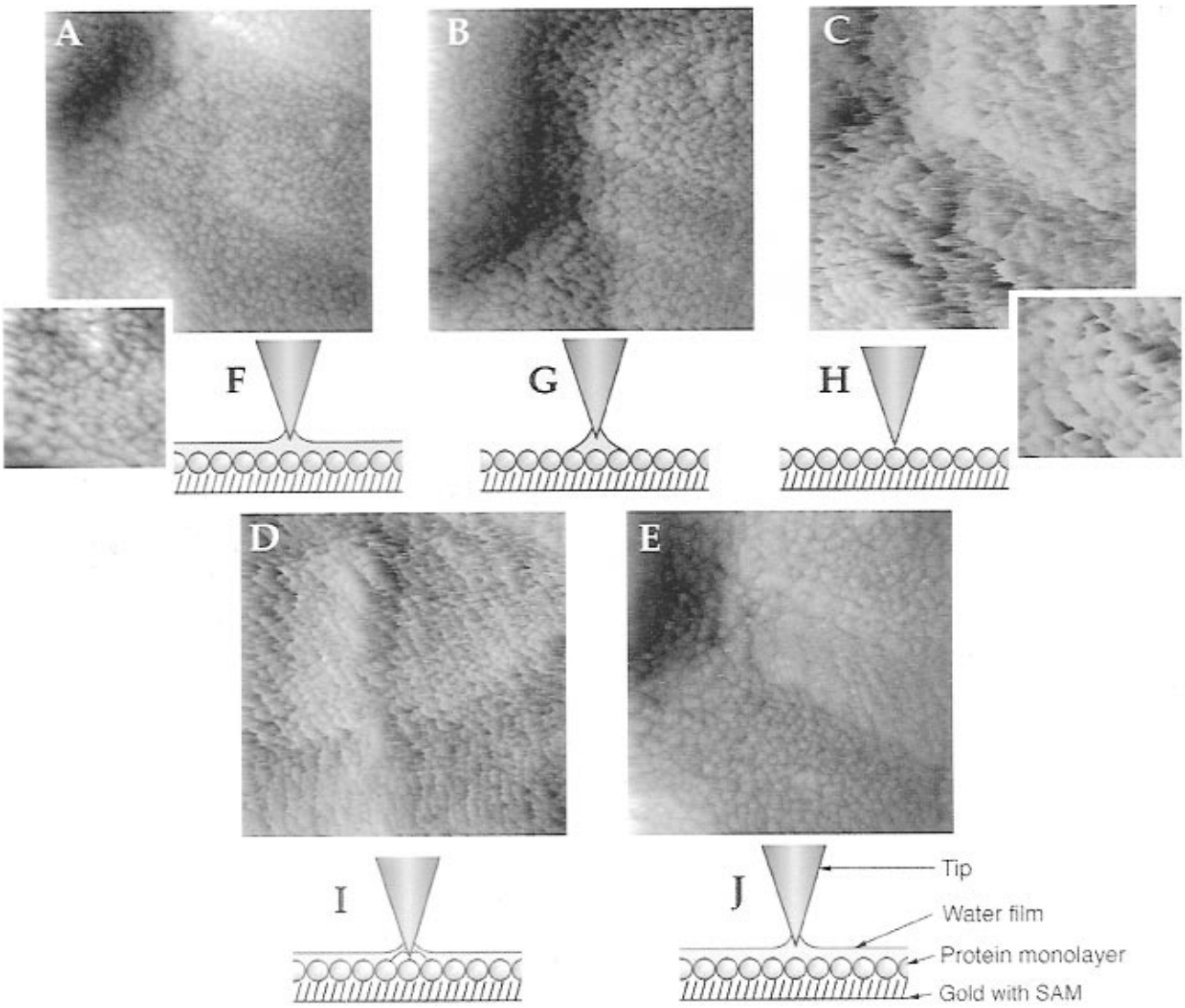

Figure 1. STM scans and proposed tip−water interaction. (A−E) STM scans (285 × 285 nm) showing the effect of controlled humidity on image contrast. (A) Immobilized catalase monolayer hydrated to 76% R.H. at 20 °C for 2 h (inset, 100 × 100 nm). (B) Monolayer dehydrated to 2% R.H. for 2 h while maintaining imaging current. (C) Tip raised then lowered, returning to the imaging state (inset, 100 × 100 nm). (D) Monolayer hydrated (76% R.H.) for 2 h while maintaining imaging current. (E) Tip raised then lowered. The tip has been maintained over the same region of the sample. Imaging conditions: imaging current 40 pA, sample bias −1.13 V, scan speed 500 nm/s. The height separations between black and white pixels are 9.9 nm (A), 13.1 nm (B), 15.4 nm (C), 10.7 nm (D), and 12.2 nm (E). (F−J) Proposed interaction of the STM tip with the adsorbed surface water. (F) Tip in contact with adsorbed water film at 76% R.H. (G) On sample dehydration (2% R.H.), there is retention of adsorbed water between tip and sample with surrounding areas dehydrated. (H) Tip retraction results in breakage of water bridge which then fails to reform on lowering of tip. (I) On sample rehydration (76% R.H.), the sharp nature of the tip and its close proximity to the sample inhibits adsorbtion of surface water under the tip. (J) Tip retraction allows formation of a continuous layer of adsorbed water, which the tip penetrates on lowering.

tip contact does not disrupt the covalently immobilized protein monolayer as shown by Figure 1E. On rehydration, failure in the restoration of image contrast suggests the tip apex fails to fully wet. Figure 1I shows a schematic illustration of a tip that is partially wetted. One possible explanation for this is that during rehydration, water can easily adsorb to the protein monolayer, but if the tip has a small radius of curvature, wetting is inhibited. At room temperature, there exists a critical radius $r_c \approx 13.8$ ln(100/R.H.) (nm) below which the tip fails to wet and remains dry.[7] Morphological analysis of the image data[12] reveals the tip having a maximum radius of curvature of 3.5 nm, which is lower than the critical radius, 3.8 nm, at 76% R.H. Failure in the wetting of the tip apex prevents formation of a continuous water film and results in poor image contrast. We have noted for STM tips with radii larger than 3.8 nm that image contrast can gradually improve due to wetting of the blunt tip during the rehydration phase. In the cases where the tip appears not to wet, retraction of the tip allows formation of a continuous water film, which the tip penetrates on lowering (Figure 1J). The partial wetting of the tip in Figure 1I could also result from the gross morphology of the tip sterically preventing wetting of the tip apex. Alternatively, a change in the tip due either to the tip stability or contamination may account for Figure 1C,D. However, we believe the latter is untrue, as provided a sharp tip is used these results have been reproducible.

Similar effects produced by hydration, dehydration and rehydration have also been demonstrated using the protein fibrinogen (Figure 2). Fibrinogen is a 340 kDa protein comprised of two terminal domains (10 nm × 6 nm) tethered to a central domain (5 nm diameter) with an overall length of 45 nm. Figure 2A displays an image of a submonolayer of fibrinogen recorded in a high-humidity environment (76% R.H.). Globular features are observed with diameters ranging from 6 to 20 nm and heights ranging from 4 to 5 nm. We believe the smaller globular features correspond to the individual molecular domains of the protein and the larger features resulting from the possible folding and compaction of the protein during preparation. Dehydration of the environment produces no

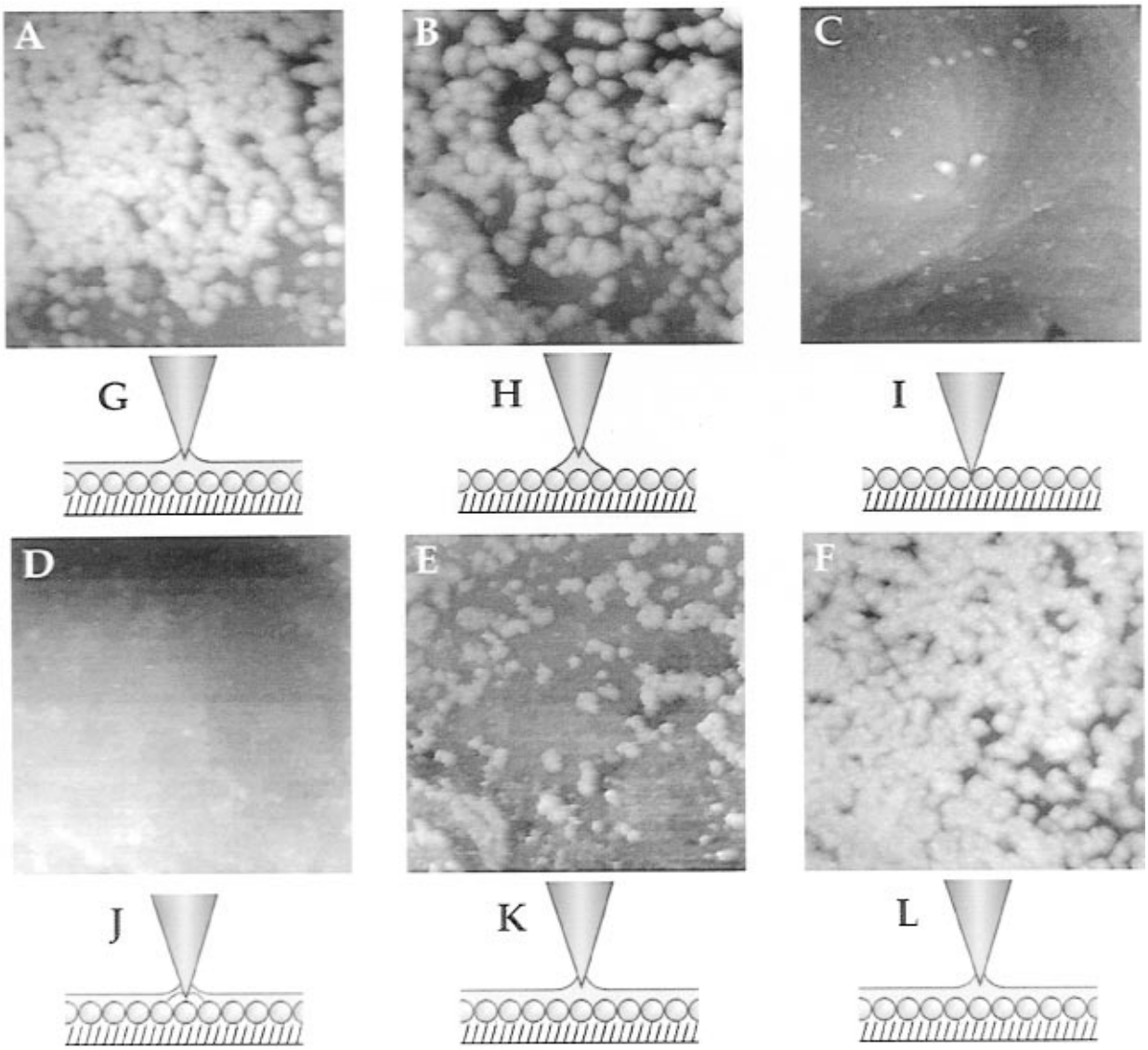

Figure 2. STM scans and proposed tip−water interaction. (A−F) STM scans (200 × 200 nm) showing the effect of controlled humidity on image contrast. (A) Immobilized fibrinogen hydrated to 76% R.H. at 20 °C for 2 h. (B) Fibrinogen dehydrated to 2% R.H. for 2 h while maintaining imaging current. (C) Tip raised then lowered, returning to the imaging state. (D) Fibrinogen hydrated (76% R.H.) for 2 h while maintaining imaging current. (E) Fibrinogen imaged repeatedly for 10 min. (F) Tip raised then lowered. Imaging conditions: imaging current 40 pA, sample bias +1.13 V, scan speed 500 nm/s. The height separations between black and white pixels are 14.8 nm (A), 14.1 nm (B), 6.7 nm (C), 8.6 nm (D), 11.5 nm (E) and 7.7 nm (F). (G−L) Proposed interaction of the STM tip with the adsorbed surface water. (G) Tip in contact with adsorbed water film at 76% R.H. (H) On sample dehydration (2% R.H.) there is retention of adsorbed water between tip and sample with surrounding areas dehydrated. (I) Tip retraction results in breakage of water bridge which then fails to reform on lowering of tip. (J) On sample rehydration (76% R.H.), wetting of the tip apex is initially inhibited. (K) Tip wetting occurs forming a continuous layer of adsorbed water during repeated imaging. (L) Tip retraction removes the tip apex from the water film. Tip lowering results in the apex penetrating the water film.

change in image contrast (Figure 2B) when the tip remains in contact with the surface. However, if the tip is retracted and lowered (Figure 2C), image contrast is significantly reduced with individual molecules no longer visible. The absence of molecules is probably due to the reduction in conductivity of the surface resulting in a decreased tip−sample separation. In Figure 2C, the underlying gold surface has been imaged. However, despite the tip contacting the protein surface, molecules appear not have been swept. Accumulated debris which often accompanies sweeping by STM tips is not present in Figure 2E or subsequent lower resolution images (not shown). On rehydration there is no improvement in image contrast initially (Figure 2D), but repeated scanning results in significant improvement in image contrast to the original level (Figure 2E) indicating the gradual wetting of the tip apex. This tendency to wet is supported by morphological analysis of the image data which reveals the tip having a maximum radius of curvature of 4.1 nm, greater than the critical radius of 3.8 nm at 76% R.H. Tip retraction and lowering produces no further improvement in image contrast (Figure 2F). From repeat experiments it has been observed the change in images between parts B and C of Figure 2 is greater than that between parts B and C of Figure 1. This may indicate that the residual conductivity of fibrinogen is lower than that of catalase. Some indication of molecular contrast still remains when imaging catalase at low humidity. This may be due to a tunneling effect involving the protein's intrinsic bound water content or possibly a resonance enhancement effect.[13]

Interpretation of the results is made more difficult if the same area of the sample is not imaged. To minimize this, the tip was maintained over the same region of the sample. Figure 1A−E shows the same region of the sample with common features seen in all five images. Sample drift has resulted in Figure 1D being offset in the $-x$ direction by approximately 150 nm. Increased sample drift between Figure 2A−F prevented the exact same area from being imaged. Therefore, to

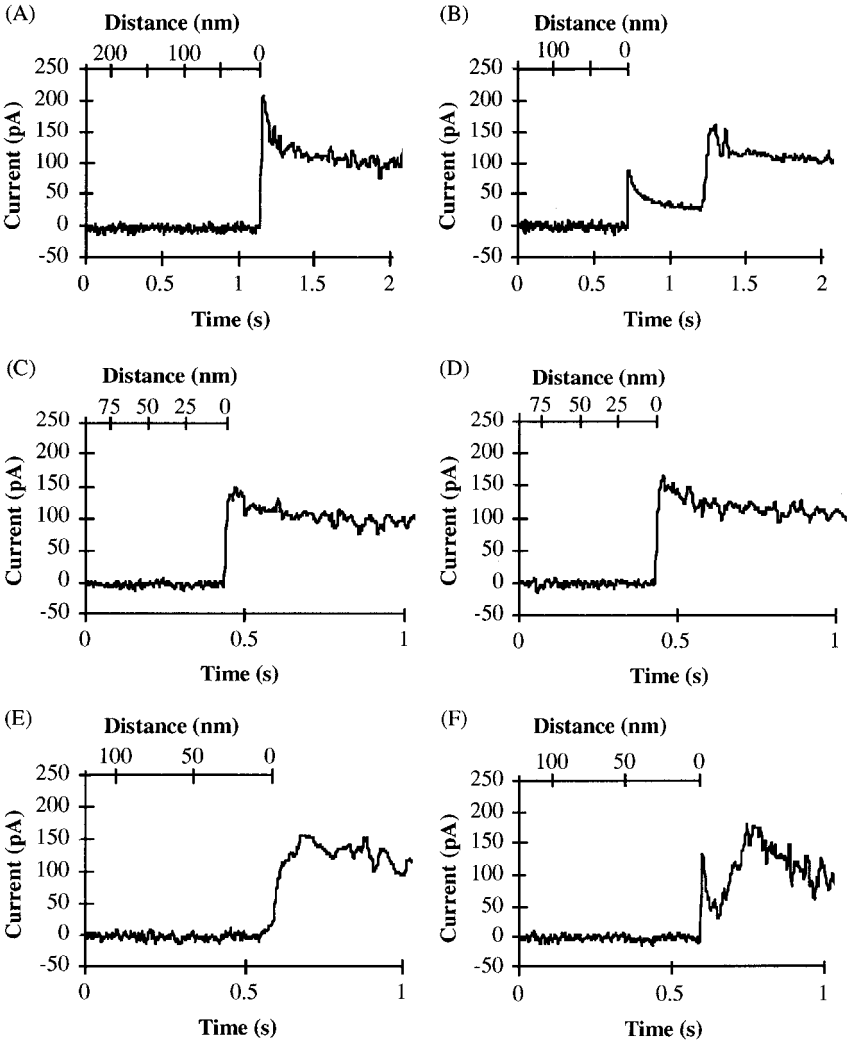

Figure 3. Current−time plots during approach of the STM tip to the sample surface in dehydrated (2% R.H.) and hydrated (76% R.H.) environments. Preset current was set at 100 pA and sample bias at +1.13 V. (A) Dehydrated and (B) hydrated Pt−C surface previously cleaned using an oxygen plasma. (C) Dehydrated and (D) hydrated bare gold surface. (E) Dehydrated and (F) hydrated fibrinogen immobilized on gold. The limited response time of the feedback circuit results in an initial current increase greater than the preset value. The subsequent decline in current shown is due to the feedback circuit retracting the tip until the preset value is reached. The *z*-movement of the tip has been translated from time to distance up until the point of current flow. Following this, the feedback circuit comes into action and the *z*-movement is no longer linear.

ensure the area imaged is representative of the occurring events, larger areas were also imaged. Parts A and B of Figure 2 are adjacent areas of the sample. Larger scan areas (not shown) reveal a uniform distribution of fibrinogen molecules as seen in Figure 2A,B. The tip retraction and lowering between parts B and C of Figure 2 resulted in greater sample drift, although from larger scan areas it is evident that parts C, D, and E of Figure 2 are of the same area. In addition, larger scan images following Figure 2E revealed areas of sparse distribution of fibrinogen; however, the molecules are separated by only a few nanometres. This confirms the absence of molecules in Figure 2C,D is a result of the image contrast mechanism. Again, tip retraction and lowering between parts E and F of Figure 2 result in sample drift leading to the imaging of an adjacent area (Figure 2F). Providing a sharp tip is used, the events that occur during hydration, dehydration, and rehydration of the protein film are reproducible.

During the presence of a water bridge, optimum image resolution depends on a minimal amount of the tip penetrating the water film. In addition, if the sample is imaged at a very high relative humidity (>76% R.H.), the water bridge may merge with the water adsorbed on the tip root leading to oscillations of the tip.[7] In our experiments, we too have have noticed these tip oscillations at higher relative humidities; however, none were observed at 76% R.H. The high resolution of the images presented in Figures 1 and 2 indicate that tip immersion is very small.

The proposed buildup of a water bridge between the STM tip and the sample surface can be detected by monitoring the current signal during tip approach.[8] Using a hydrated glow discharged Pt−C surface Guckenberger *et al.* have demonstrated that with picoampere currents a water bridge can form. In addition, they have demonstrated a failure of water bridge formation on hydrated bare gold or mica. This resulted in their conclusion that charge transfer between tip and hydrated mica is based on a tunneling mechanism. Using a similar approach, we have investigated the water bridge formation on the above protein surface in high- and low-humidity environments. Figure 3A,B displays current−time plots recorded on approach to a Pt−C surface cleaned with an oxygen plasma. The plasma cleaning renders the surface highly hydrophilic (measured water contact angle less than 10°). In a low-humidity environment (2% R.H.), the STM tip approaches the surface and attains the preset current, as shown in Figure 3A as a sharp rise in current. Following rehydration of the environment to 76% R.H., water is readily adsorbed to this hydrophilic surface and enables a water bridge to form during tip approach. Penetration of the tip into the surface water results in an initial current surge, as

indicated in Figure 3B. The secondary current increase in Figure 3B is a result of the tip continuing to approach into the water film until the preset current value is established.[8] Figure 3C,D displays current−time plots recorded on approach to a bare gold surface. In a low-humidity environment, tunneling occurs on tip approach as for the Pt−C surface (Figure 3C). However, following rehydration of the environment, a single sharp rise in current during approach indicates that tunneling is attained without the formation of a water bridge. This can be attributed to gold having a more hydrophobic surface than the Pt−C (water contact angle: 72° ± 2°), which discourages the adsorption of a water film. Current−time plots recorded on approach to dehydrated fibrinogen immobilized on gold (Figure 3E) show an absence in the formation of a water bridge. An initial gradual increase in current is observed which may indicate the tip comes into contact with the protein surface before the set point current is reached. However, on hydration (Figure 3F) an initial current surge is again observed followed by a gradual increase in current which stabilizes at the preset value. This data indicates that, as in the case of Pt−C, the approaching tip penetrates the adsorbed surface water on fibrinogen creating a water bridge. This is supported by the fibrinogen covered surface being more hydrophilic (contact angle: 47° ± 2°) as is the underlying SPDP monolayer (contact angle: 33° ± 2°), hence promoting water adsorption at high humidities and increasing the likelihood of a water bridge formation.

These findings clearly indicate penetration of the STM tip apex into the adsorbed surface water on protein monolayers. We believe this strongly suggests the mechanism of charge transfer between tip and surface, and hence image formation during hydration is in part electrochemical in nature as concluded by Fan and Bard.[1] The charge transfer involves cations and anions in the water film with redox reactions involving water also occurring. However, it is worthy to note that even when imaging at low humidity (<2% R.H.) some indication of molecular contrast can remain. This may be due to an additional tunneling effect involving the protein's intrinsic bound water content or possibly a resonance enhancement effect.[13]

To conclude, this data strongly supports the critical role of water in the STM contrast mechanism for proteins. Using two different protein monolayers, clear evidence for the STM tip penetrating an ultrathin adsorbed water film on hydrated samples has been provided.

Acknowledgment. M.C.D., C.J.R., and S.J.B.T. acknowledge the funding of a studentship by Eli Lilly (for N.P.), the support of a DTI-EPSRC Nanotechnology LINK Scheme in collaboration with Kodak Limited, Oxford Molecular plc, and Fisons Instruments (for M.L. and P.M.W.), and the Royal Society for the funding of a gold evaporator.

References and Notes

(1) Fan, F.-R. F.; Bard, A. J. *Science* **1995**, *270*, 1849. This is a comment to ref 2 and includes a response from the authors of ref 2.
(2) Guckenberger, R.; Heim, M.; Cevc, G.; Knapp, H. F.; Wiegräbe, W.; Hillebrand, A. *Science* **1994**, *266*, 1538.
(3) Parker, M. C.; Davies, M. C.; Tendler, S. J. B. *J. Phys. Chem.* **1995**, *99*, 16155.
(4) Leggett, G. J.; Davies, M. C.; Jackson, D. E.; Roberts, C. J.; Tendler, S. J. B.; Williams, P. M. *J. Phys. Chem.* **1993**, *97*, 8852.
(5) Maaloum, M.; Chretein, D.; Karsenti, E.; Hörber, J. K. H. *J. Cell Sci.* **1994**, *107*, 3127.
(6) Guckenberger, R.; Teran-Arce, F.; Hillebrand, A.; Hartmann, T. *J. Vac. Sci. Technol. B* **1994**, *12*, 1508.
(7) Yuan, J-Y.; Shao, Z.; Gao, C. *Phys. Rev. Lett.* **1991**, *67*, 863.
(8) Heim, M.; Eschrich, R.; Hillebrand, A.; Knapp, H. F.; Guckenberger, R. *J. Vac. Sci. Technol. B* **1996**, *14* (2), 1498.
(9) Nuzzo, R. G.; Allara, D. L. *J. Am. Chem. Soc.* **1983**, *105*, 4481.
(10) Murthy, M. R. N.; Reid, T. J., III.; Sicignano, A.; Tanaka, N.; Rossmann, M. G. *J. Mol. Biol.* **1981**, *152*, 465.
(11) Crassous, J.; Charlaix, E.; Gayvallet, H.; Loubet, J-L. *Langmuir* **1993**, *9*, 1995.
(12) Williams, P. M.; Shakesheff, K. M.; Davies, M. C.; Jackson, D. E.; Roberts, C. J.; Tendler, S. J. B. *Langmuir* **1996**, *12*, 3468.
(13) Lindsay, S. M.; Sankey, O. F.; Li, Y.; Herbst, C. *J. Phys. Chem.* **1990**, *94*, 4655.